

Influence of Arterial Occlusion at Various Cuff Pressures on Systemic Circulation Measured by rPPG

Leah De Vos¹, Gennadi Saiko²^a, Denis Bragin^{3,4}^b and Alexandre Douplik^{2,5}^c

¹Department of Engineering, Toronto Metropolitan University, Toronto, Canada

²Department of Physics, Toronto Metropolitan University, Toronto, Canada

³Lovelace Biomedical Research Institute, Albuquerque, U.S.A.

⁴Department of Neurology, University of New Mexico School of Medicine, Albuquerque, U.S.A.

⁵iBest, Keenan Research Centre of the LKS Knowledge Institute, St. Michael's Hospital, Canada

Keywords: Photoplethysmography, Arterial Occlusion, Microcirculation.

Abstract: *Background:* Arterial occlusion is a ubiquitous medical procedure, which is used in many clinical scenarios. However, there is no standard protocol for the selection of the applied pressure. As various pressures may trigger different physiological responses, it is important to understand these peculiarities. The aim of the current work is to investigate if there is any difference in the systemic response to the occlusion at various applied pressures. *Methods:* Hands of healthy volunteers (10 volunteers) were occluded at the wrist by inflating the blood cuff to 150 or 200 mmHg. The remote photoplethysmography (rPPG) measurements of control and experimental hands were taken. To assess systemic response, we have analysed the behaviour of AC (low frequency, LF at 0.1 Hz rate) components in green and red channels during occlusion and reperfusion. *Results:* We have not found a statistically significant difference in the LF spectra between occlusions at 150 and 200 mmHg pressures. *Conclusions:* We have performed the analysis of low-frequency (0.1 Hz) components of remote photoplethysmography signals during arterial occlusion at 150 and 200 mmHg. Our preliminary results show that the systemic response is similar at both levels of occlusions.


1 INTRODUCTION


Arterial occlusion is a ubiquitous medical procedure. It is used in many clinical scenarios. Probably the most well-known use of arterial occlusion is blood pressure measurements using an auscultatory method, which was originally based on a stethoscope and a sphygmomanometer. Another important clinical use of arterial occlusion is to detect endothelial dysfunction in critically ill patients (Joannides et al., 2006).


In common clinical scenarios the arterial occlusion is caused by placing the blood pressure cuff over the forearm or wrist and inflating it over systolic blood pressure (Lenders et al., 1991). Common sense would suggest that inflating the blood cuff just over systolic pressure would be sufficient to occlude arteries of the hand. However, it is not the case.

As a rule, an additional pressure of 50 mmHg is typically considered to be a safe margin (Kanchanathepsak et al., 2023). However, the exact relationship between the applied pressure and the level of occlusion is not well understood and established in the literature. In particular, it can be driven by multiple factors such as BMI. As such, the applied pressure often is a tradeoff between the desire to occlude vessels and patient's tolerance to pain. The latter is particularly important for a bed-side test for endothelial dysfunction assessment, where the artery is occluded for 3 min (Saldin, 2019). Thus, it could be beneficial to get more insights into the differences at various levels of the occlusion. Such investigation can be based on observing hemodynamic response, which can be on a local and systemic level.

Remote photoplethysmography (rPPG) has been shown its utility in investigation of skin

 <https://orcid.org/0000-0002-5697-7609>

 <https://orcid.org/0000-0003-4894-0061>

 <https://orcid.org/0000-0001-9948-9472>

microcirculation (Burton et al., 2023). The predominant signal source in the PPG is the cardiac pulsation caused by the ejection of blood from the left ventricle during cardiac systole, which causes distensions of blood vessels and changes in the tissue absorption. These blood waveforms demonstrate changes in five frequency bands, which are related to different physiological processes. Heart rate for normal subjects at rest varies from 60-100 beats per minute (bpm) (*Vital Signs (Body Temperature, Pulse Rate, Respiration Rate, Blood Pressure)*, 2022). Conservatively extending the lower bound to 50 bpm to consider lower resting heart rates that can occur in certain people, such as athletes (Doyen et al., 2019), then the corresponding frequency range is 0.83-1.67 Hz. The normal respiration rate for a healthy subject is 12 to 20 breaths per minute, corresponding to a frequency range of 0.20-0.33 Hz (*Vital Signs*, n.d.). This PPG signal further contains oscillations in 0.01-0.02 Hz, 0.02-0.06 Hz, 0.06-0.15 Hz ranges corresponding to endothelial related metabolic, neurogenic, and myogenic activities, respectively (Li et al., 2006). Myogenic range also contains Mayer waves, which are oscillations in blood pressure that typically occur at a frequency of 0.1 Hz (Julien, 2006). The mechanism for Mayer waves is subject to active debate, but recent findings advocate that the oscillations are produced by a sympathetic baroreceptor response to hemodynamic disturbances (Julien, 2006). The ability to capture Mayer waves by a smartphone camera was demonstrated in (Burton et al., 2022). As occlusion and/or reperfusion may trigger hemodynamic disturbance we hypothesize that this disturbance can depend on the severity of occlusion/reperfusion and characterize this difference.

The aim of the current work is to investigate the differences in systemic physiological response to the occlusion/reperfusion at various applied pressures. We used rPPG to analyze skin microcirculation in an arterial occlusion model with 2 different applied pressures. We have selected 150 mmHg as a pressure which is just marginally higher than the systolic pressure, and 200 mmHg, as a higher pressure with 50 mmHg safety margin. As we aim to investigate the systemic response, we have analyzed the rPPG signal in both experimental and control hands.

2 METHODS

2.1 Data Collection

The experimental setup, as seen in Figure 1, includes the subject sitting with their hands placed side by side

on a raised platform in the prone position. An iPhone 14 camera (Apple, Cupertino, CA, USA) is held by a tripod above the hands positioned directly above. As a light source, two rectangular video light panels with 600 LEDs on each panel (NEEWER LED Video Light, Shenzhen, China) were positioned on either side of the camera illuminating the hands (light colour was set to 4600K to maximize the green channel signal and 100% intensity was set to ensure maximum signal to noise ratio). A white circle of 1 cm diameter is also placed in the frame next to the hands for colour normalization during processing. In each iteration of data collection, one hand is designated as the experimental hand, occluded throughout the data collection, and the other acts as a control. On the arm of the experimental hand, a pressure cuff is worn around the wrist to apply pressure during the data collection.



Figure 1: Experimental setup. (From top to bottom) LED panels, iPhone 14, pressure cuff and hands placed on staging table.

Once the setup is established, the data collection procedure is as follows:

1. The subject's initial blood pressure is measured from the experimental arm.
2. The subject places both hands on the platform, in the prone position. At this point, the iPhone starts recording video at 60 fps.
3. Baseline measurements are recorded for 1 minute (baseline interval).

4. Arterial occlusion is then applied on the experimental hand for 3 minutes by applying 150 mmHg of pressure (occlusion interval).
5. The pressure is then released and no pressure is applied to the arm for 4 minutes (reperfusion interval).
6. At the 8-minute mark data collection concludes and the iPhone recording video and the muscle oxygenation monitor are both turned off.

A rest period of 5 minutes is taken and then the process is repeated for steps 2-6 with the opposite arm acting as the experimental hand and with 200 mmHg of pressure being applied instead of 150 mmHg.

For this work, data from 10 subjects were acquired (age range: 20-60 years old, 4 males, 6 females) each with no evidence of cardiovascular disease and no extreme BMI values. The Toronto Metropolitan Research Ethical Board approved this study.

2.2 Image Processing

The recorded video footage from the data collection is then processed and analysed using MATLAB 2023b (Mathworks, Natick, MA, USA). First, to improve processing time, the video is cut into three segments each representing sequentially no pressure, arterial occlusion (150 mmHg or 200 mmHg) and pressure release. The following processing is applied to each video segment. A Gaussian filter is applied to each video frame to reduce the amount of noise in the video and high-frequency components in the video. Next, three regions of interest (ROI) are manually selected from the video file, one on the experimental hand, one on the control hand and one around the white circle. For each ROI, each video frame's pixels are averaged for each colour channel (red, green and blue (RGB)) resulting in a single red, green and blue value per frame. This creates signals representing a time series for each colour channel. To normalize the time series for the experimental and control hands the following equations are used,

$$e_{i,j} = 255 \frac{E_{i,j}}{R_{i,j}} \quad (1)$$

$$c_{i,j} = 255 \frac{C_{i,j}}{R_{i,j}} \quad (2)$$

Where i refers to the colour channel ($i = \text{red, green, and blue}$), j refers to the frame's number ($j = 1 - N$, where N is the number of frames), E represents the experimental hand time series, C represents the

control hand times series and R represents the white circle time series.

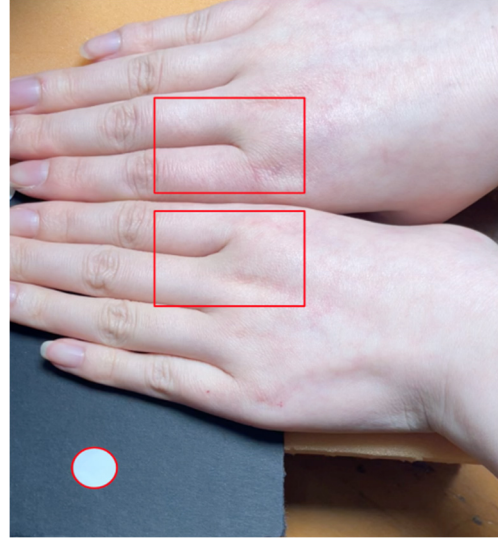


Figure 2: Experiment hand placements, and highlighted regions of interest in red.

2.3 Data Analysis

The DC component of the signal represents the average intensity of the signal over time and the AC component represents changes in the signal associated with the cardiac cycle. For this work, we considered the AC component of the signal. As such, for AC component of the rPPG signal, changes in amplitude over time due to arterial occlusion events were analysed, specifically amplitude drop relative to baseline condition when occlusion is applied and the amplitude overshoot relative to baseline when the pressure is released. The calculations performed for each component are as follows:

2.3.1 AC Component

For the AC component, the low frequency range in the red and green channels were analysed. To retrieve the LF spectral range, each channel was run through a bandpass filter with a frequency range of 0.05-5 Hz. After the signals are filtered to this frequency range, the continuous wavelet transforms (CWT) is applied on the signals calculating the mean power of the results. After this the power spectral density (PSD) in the LF range for both the red and green channels can be calculated. To express the percent drop of the LF frequency of the experimental hand relative to the control hand when pressure is applied and the overshoot when pressure is released, the following equation is used,

$$\% \text{ change} = \frac{\text{value}_i - \text{baseline}}{\text{baseline}} \times 100 \quad (3)$$

Where i represents the segment number ($i = 2-3$), value_i represents the PSD value at 0.1 Hz on occlusion ($i=2$) or reperfusion ($i=3$) segment, and baseline represents the PSD value at 0.1 Hz on baseline ($i=1$) segment. The above equation was performed on both the red and green channels for each segment, and for experimental and control hands.

2.3.2 Statistical Analysis

To assess the statistical significance of the differences between results, i.e. comparing between AC components, two-tailed t-tests were performed. In this case the null hypothesis was that the mean of data 1 is equal to the mean of data 2, essentially that there is no significant difference between the two datasets. The alternative hypothesis is that the mean of data 1 is not equal to the mean of data 2 denoting a significant difference between the two datasets. To perform the t-test, the following process is followed. First the t-test statistic is calculated as,

$$t = \frac{\bar{x}_1 - \bar{x}_2}{\sqrt{\frac{s_1^2}{n_1} + \frac{s_2^2}{n_2}}} \quad (4)$$

Where \bar{x}_1 and \bar{x}_2 are the means of data 1 and data 2 respectively, s_1 and s_2 are the standard deviations of data 1 and data 2 respectively, and n_1 and n_2 are the sample sizes of data 1 and data 2 respectively. Then the p-value is determined by first calculating the degree of freedom by,

$$df = \frac{\left(\frac{s_1^2}{n_1} + \frac{s_2^2}{n_2}\right)^2}{\left(\frac{s_1^2/n_1}{n_1-1}\right) + \left(\frac{s_2^2/n_2}{n_2-1}\right)} \quad (5)$$

Once df is calculated then the p-value can be found as,

$$p - \text{value} = P(T > t \mid df) \quad (6)$$

Where T is the random variable following a t-distribution with df and t is the test statistic. From there if the p-value $< \alpha$ (significance level set as $\alpha = 0.05$) the null hypothesis is rejected and if the p-value $\geq \alpha$ the null hypothesis is accepted. For this study the computations were performed in MATLAB.

3 RESULTS

We have analysed the behaviour of the AC components at LF spectral range in green and red channels during occlusion and overshoot. The results are depicted in Figure 3 and Figure 4, respectively. The results are also summarized in Table 1 for the experimental hand and Table 2 for the control hand.

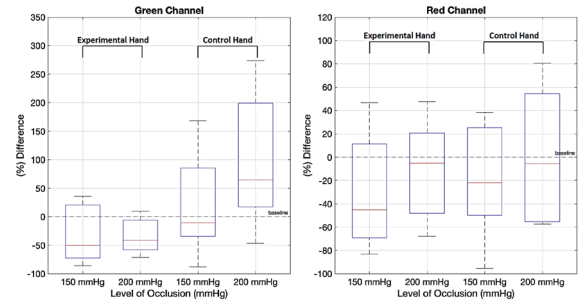


Figure 3: The behaviour of AC components in green (left panel) and red (right panel) channels during occlusion. The drop has been calculated as a relative change in AC component on the 2nd interval compared to the baseline.

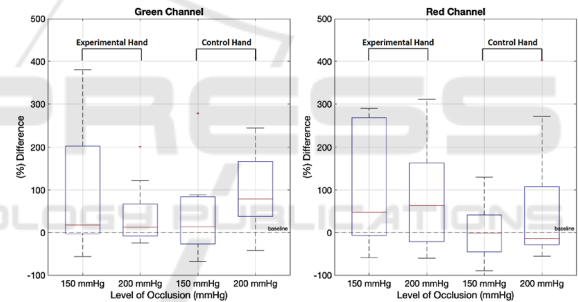


Figure 4: The behaviour of AC components in green (left panel) and red (right panel) channels during reperfusion. The overshoot has been calculated as a relative change in AC component on the 3rd interval compared to the baseline.

Table 1: Comparison of different metrics at 150 and 200 mmHg on the experimental hand. Specifically mean, standard deviation (in brackets), and p-value (with significance noted by (ns), no statistical significance, when $p > 0.05$).

Metric	Mean @ 150 mmHg	Mean @ 200 mmHg	p-value
Reperfusion Red Channel	155.26 (268.91)	84.69 (122.72)	0.46 ^(ns)
Reperfusion Green Channel	92.18 (158.02)	38.60 (72.34)	0.34 ^(ns)
Occlusion Red Channel	-15.91 (82.94)	-10.51 (43.26)	0.86 ^(ns)
Occlusion Green Channel	-32.80 (47.77)	-34.30 (27.79)	0.93 ^(ns)

Table 2: Comparison of different metrics at 150 and 200 mmHg on the control hand. Specifically mean, standard deviation (in brackets), and p-value (with significance noted to (ns), no statistical significance, when $p > 0.05$).

Metric	Mean @ 150 mmHg	Mean @ 200 mmHg	p-value
Reperfusion Red Channel	3.70 (67.42)	68.15 (155.25)	0.244 ^(ns)
Reperfusion Green Channel	35.05 (99.15)	118.91 (129.85)	0.12 ^(ns)
Occlusion Red Channel	-6.18 (72.96)	24.19 (111.01)	0.48 ^(ns)
Occlusion Green Channel	20.57 (80.03)	93.23 (102.29)	0.09 ^(ns)

4 DISCUSSION

Here, we present an initial pilot investigation of the microvasculature hemodynamic during occlusion/reperfusion captured by a smartphone camera. Data was collected as described from ten healthy subjects. We have performed the analysis of remote photoplethysmography signals in the low frequency (0.1 Hz) range for two levels of occlusion: mild occlusion (150 mmHg) and occlusion with a safety margin (200 mmHg).

As we aimed to investigate the systemic response, we analyzed the rPPG signal in both the experimental and control hands.

The behaviour of the LF component is very similar for both levels of occlusion. In particular, we have not found any statistically significant differences between distributions caused by 150 and 200 mmHg either during occlusion or reperfusion.

During occlusion, AC amplitudes in the experimental hand in the 0.1 Hz range drop for both 150 and 200 mmHg pressures (see Figure 3). The drop distributions are characterized by very similar means and standard deviations. It holds true for both the green and red channels.

During occlusion, AC amplitudes in the control hand in the 0.1 Hz range increase for both 150 and 200 mmHg pressures in the green channel (see Figure 3). The increase distributions are characterized by very similar means and standard deviations. It holds true for both green and red channels.

During reperfusion, the behaviour of the 0.1 Hz range component in the experimental hand in 150 and 200 mmHg cases are also characterized by very similar means. However, standard deviations for 150 and 200 mmHg pressures are quite different in both red and green channels (see Figure 4).

Moreover, during reperfusion, one can see that there is a substantial (by 50-70% in red channel)

increase in 0.1 Hz oscillations in the experimental hand.

We hypothesize that these low-frequency oscillations can be attributed to Mayer waves. While Mayer waves share the same frequency range as myogenic activities (0.06-0.15Hz), their origins are different. Mayer waves are the sympathetic activity with baroreflex activation. Myogenic oscillations are local and independent of the sympathetic nervous vasoconstriction.

Our conclusion regarding the origin of the 0.1 Hz amplitude increase is based on two observations. Firstly, we see similar results during reperfusion in both experimental and control hands. Thus, it speaks in favour of systemic response. Secondly, the results are quite similar for red and green channels, which have different sampling depth. Thus, similarity in these responses also points in favour of Mayer waves, as local regulation should demonstrate some differences between capillary network (sampled by the green channel) and deep vascular plexus (sampled by the red channel).

Thus, we can conclude that both lower and higher pressures are probably triggering a similar systemic response in the form of a sympathetic baroreceptor response to hemodynamic disturbances.

The work has certain limitations. Firstly, the measurements were performed on just 10 participants. Thus, larger studies are required to generalize the results. Secondly, the short time interval (5 min) between the measurements on left (150 mmHg occlusion) and right (200 mmHg occlusion) hands was taken. While quite a significant amount of time was allowed for baseline and reperfusion measurements (1 and 4 min, respectively), it potentially still may impact the blood flow in the control (left) hand during 200 mmHg occlusion of the right hand. To mitigate this risk, more time (e.g. 10 min) needs to be allowed between experiments in future.

In future work we plan to compare rPPG with contact PPG, which also measures microcirculation in skin, and investigate other frequency ranges.

5 CONCLUSIONS

We have performed the analysis of low-frequency (0.1 Hz) components of remote photoplethysmography signals during arterial occlusion and reperfusion at 150 and 200 mmHg. Our preliminary results show that the systemic response is similar at both levels of occlusions.

ACKNOWLEDGEMENTS

We would like to thank the volunteers who participated in our study, without whom our work would not have been possible. The authors acknowledge funding from NSERC Alliance (A.D), NSERC Personal Discovery (A.D. and G. S.), and Toronto Metropolitan University Faculty of Science Discovery Accelerator program (G.S.).

Minute Reactive Hyperemia. *Master's Theses*. <https://doi.org/10.15368/theses.2019.4>
Vital Signs (Body Temperature, Pulse Rate, Respiration Rate, Blood Pressure). (2022, June 14). <https://www.hopkinsmedicine.org/health/conditions-and-diseases/vital-signs-body-temperature-pulse-rate-respiration-rate-blood-pressure>
Vital Signs: How to Check My Vitals at Home. (n.d.). Cleveland Clinic. Retrieved November 21, 2023, from <https://my.clevelandclinic.org/health/articles/10881-vital-signs>

REFERENCES

- Burton, T., Saiko, G., Cao, M., & Douplik, A. (2023). Remote photoplethysmography with consumer smartphone reveals temporal differences between glabrous and nonglabrous skin: Pilot in vivo study. *Journal of Biophotonics*, *16*(1), e202200187. <https://doi.org/10.1002/jbio.202200187>
- Burton, T., Saiko, G., & Douplik, A. (2022). Remote PPG Imaging by a Consumer-grade Camera under Rest and Elevation-invoked Physiological Stress Reveals Mayer Waves and Venous Outflow: *Proceedings of the 15th International Joint Conference on Biomedical Engineering Systems and Technologies*, 153–159. <https://doi.org/10.5220/0010883100003123>
- Doyen, B., Matelot, D., & Carré, F. (2019). Asymptomatic bradycardia amongst endurance athletes. *The Physician and Sportsmedicine*, *47*(3), 249–252. <https://doi.org/10.1080/00913847.2019.1568769>
- Joannides, R., Bellien, J., & Thuillez, C. (2006). Clinical methods for the evaluation of endothelial function – a focus on resistance arteries. *Fundamental & Clinical Pharmacology*, *20*(3), 311–320. <https://doi.org/10.1111/j.1472-8206.2006.00406.x>
- Julien, C. (2006). The enigma of Mayer waves: Facts and models. *Cardiovascular Research*, *70*(1), 12–21. <https://doi.org/10.1016/j.cardiores.2005.11.008>
- Kanchanathepsak, T., Pukrittayakamee, N. C., Woratanarat, P., Tawonsawatruk, T., & Angsanuntsukh, C. (2023). Limb occlusion pressure versus standard tourniquet inflation pressure in minor hand surgery: A randomized controlled trial. *Journal of Orthopaedic Surgery and Research*, *18*(1), 539. <https://doi.org/10.1186/s13018-023-04000-3>
- Lenders, J., Janssen, G. J., Smits, P., & Thien, T. (1991). Role of the wrist cuff in forearm plethysmography. *Clinical Science (London, England: 1979)*, *80*(5), 413–417. <https://doi.org/10.1042/cs0800413>
- Li, Z., Leung, J. Y., Tam, E. W., & Mak, A. F. (2006). Wavelet analysis of skin blood oscillations in persons with spinal cord injury and able-bodied subjects. *Archives of Physical Medicine and Rehabilitation*, *87*(9), 1207–1212; quiz 1287. <https://doi.org/10.1016/j.apmr.2006.05.025>
- Saldin, T. (2019). Assessing Endothelial Dysfunction Estimating the Differences Between 3 Minute and 5